Environmental Science & Technology

pubs.acs.org/est

Article

Ozonolysis of α-Pinene and Δ^3-Carene Mixtures: Formation of Dimers with Two Precursors

Ditte Thomsen, Lotte Dyrholm Thomsen, Emil Mark Iversen, Thurídur Nótt Björgvinsdóttir, Sofie Falk Vinther, Jane Tygesen Skønager, Thorsten Hoffmann, Jonas Elm, Merete Bilde, and Marianne Glasius*

Cite This: *Environ. Sci. Technol.* 2022, 56, 16643−16651

Read Online

ACCESS | Metrics & More | Article Recommendations | Supporting Information

ABSTRACT: The formation of secondary organic aerosol (SOA) from the structurally similar monoterpenes, α-pinene and Δ^3-carene, differs substantially. The aerosol phase is already complex for a single precursor, and when mixtures are oxidized, products, e.g., dimers, may form between different volatile organic compounds (VOCs). This work investigates whether differences in SOA formation and properties from the oxidation of individual monoterpenes persist when a mixture of the monoterpenes is oxidized. Ozonolysis of α-pinene, Δ^3-carene, and a 1:1 mixture of them was performed in the Aarhus University Research on Aerosol (AURA) atmospheric simulation chamber. Here, ∼100 ppb of monoterpene was oxidized by 200 ppb O_3 under dark conditions at 20 °C. The particle number concentration and particle mass concentration for ozonolysis of α-pinene exceed those from ozonolysis of Δ^3-carene alone, while their mixture results in concentrations similar to α-pinene ozonolysis. Detailed offline analysis reveals evidence of VOC-cross-product dimers in SOA from ozonolysis of the monoterpene mixture: a VOC-cross-product dimer likely composed of the monomeric units *cis*-caric acid and 10-hydroxy-pinonic acid and a VOC-cross-product dimer ester likely from the monomeric units caronaldehyde and terpenylic acid were tentatively identified by liquid chromatography-mass spectrometry. To improve the understanding of chemical mechanisms determining SOA, it is relevant to identify VOC-cross-products.

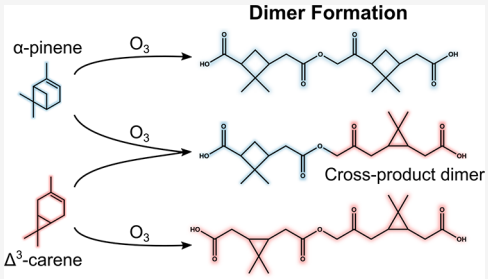

KEYWORDS: *secondary organic aerosol, sequential spot sampler, aerosol formation, monoterpene oxidation*

Downloaded via AARHUS UNIV on December 6, 2022 at 17:10:06 (UTC).
See https://pubs.acs.org/sharingguidelines for options on how to legitimately share published articles.

■ INTRODUCTION

The formation of secondary organic aerosol (SOA) in the atmosphere is important for both climate[1,2] and human health.[1,3,4] Biogenic volatile organic compounds (BVOCs) are important precursors of SOA.[1] Ozonolysis of BVOCs is widely studied in atmospheric simulation chambers, where atmospheric processes may be isolated and studied under various atmospheric conditions.[5−12] One of the most studied monoterpenes is α-pinene,[5,6,8−11,13−15] and it is often used as a model compound for the formation of SOA from endocyclic BVOCs,[16] while other monoterpenes such as Δ^3-carene have received much less attention.[12,13,17] Previous work from the Aarhus University Research on Aerosol (AURA) chamber shows that despite the similarities in the chemical structures of α-pinene and Δ^3-carene, the formation of SOA from ozonolysis of them differs substantially.[12] For the same initial concentrations of organic precursor and ozone, dark ozonolysis of α-pinene results in higher particle number concentrations and a diverse oxidation product distribution, while ozonolysis of Δ^3-carene results in higher particle mass concentrations and larger particle sizes but with significantly fewer oxidation products.[12] In recent years, research on BVOC mixtures has advanced,[18−20] but potential synergistic effects on SOA yields and properties are still not fully elucidated. McFiggans et al.[20] found that simultaneous oxidation of α-pinene and isoprene results in a decrease in SOA yields compared to the monoterpene system without isoprene present, while Ahlberg et al.[18] and Faiola et al.[19] found that complex and nonideal mixing of monoterpenes and sesquiterpenes enhance the SOA mass formation in comparison to isolated monoterpene systems. The particle phase consists of innumerable different products,[21] where especially the chemical composition of dimers may be susceptible to change in a VOC mixture. Dimers have been identified in both ambient and laboratory-generated SOA from α-pinene and Δ^3-carene[12,22,23] and may be important for new particle formation.[24,25] Dimers have been hypothesized to form through esterification of two monomeric units,[26−28] through oligomerization in the particle phase,[29,30]

Received: July 7, 2022
Revised: October 19, 2022
Accepted: October 26, 2022
Published: November 10, 2022

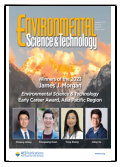

ACS Publications © 2022 American Chemical Society

Table 1. Experimental Conditions for the Experiments Performed with α-Pinene, Δ^3-Carene, and the 1:1 Mixture of α-Pinene and Δ^3-Carene Reported after Wall Loss Correction

date (yymmdd)	VOC	VOC_{max} (ppb)	$[O_3]_0$ (ppb)	T (°C)	RH (%)	maximum concentrations number ($\times 10^4$ # cm^{-3})	maximum concentrations mass (μg m^{-3})	SOA yield
210706	α-pinene	126	200	20.23 ± 0.02	1.3 ± 1.6	11.8	251	0.27
210708	Δ^3-carene	100	224	20.23 ± 0.02	0.8 ± 1.4	7.2	198	0.28
210713	mixed	119	218	20.21 ± 0.03	0.8 ± 1.3	8.4	242	0.27
210923	α-pinene	–[a]	208	20.19 ± 0.02	0.7 ± 1.2	6.2	232	0.32
211007	Δ^3-carene	–[a]	220	20.19 ± 0.08	0.2 ± 0.4	5.6	167	0.24
211012	mixed	–[a]	217	20.22 ± 0.02	0.1 ± 0.3	6.2	232	0.27

[a]Not measured with proton-transfer reaction quadrupole mass spectrometer (PTR-QMS) and calculated as 100 ppb, based on the injected volume.

or through peroxy radical dimerization in the gas phase.[31,32] Hitherto, it remains unclear whether precursor cross-product dimers exist when a mixture of VOCs is oxidized, as it has been hypothesized.[31,32] It is important to investigate whether these exist to fully characterize reactions and important compounds contributing to the aerosol.

In this work, SOA is generated from dark ozonolysis of α-pinene, Δ^3-carene, and their 1:1 mixture in the AURA atmospheric simulation chamber at 20 °C, dry conditions. Our focus is the chemical composition of the particle-phase species, in particular, carboxylic acids and cross-products containing the carbon backbone of two monomeric carboxylic acids. We refer to such cross-products tentatively identified in the particle phase as dimers, and we refer to dimers containing monomeric backbone units derived from two different VOC precursors as VOC-cross-product dimers. The SOA is collected at different times after formation and analyzed chemically using offline analysis. The AURA chamber is operated in batch mode, allowing for studies of both the initially formed products as well as the aged products in the particle phase. To avoid artifacts from filter-based aerosol sampling such as adsorption of gases leading to overestimation of the particle component concentrations[33,34] and to minimize labor and time consumption, we here use a sequential spot sampler (3S)[35] for aerosol collection. The 3S operates by activating particles with a temperature-moderated water condensation approach[36] and depositing them into wells on a multi-well plate, yielding a concentrated spot of aerosols ready for analysis.[35] In this way, the 3S provides time-resolved filter-free aerosol sampling for offline analysis. Previous studies have implemented the 3S approach with flow tube setups,[37,38] but to the best of our knowledge, this work is the first use of a sequential spot sampler for time-resolved chemical characterization in combination with chromatography of aerosol samples from atmospheric climate chambers.

■ MATERIALS AND METHODS

Dark ozonolysis experiments of α-pinene (Sigma-Aldrich, 98%), Δ^3-carene (Sigma-Aldrich, ≥98.5%), and a 1:1 mixture based on mixing ratios were performed in the AURA atmospheric simulation chamber. AURA consists of a ∼5 m^3 Teflon bag suspended from a metal frame inside a temperature-controlled room. A detailed description of the specifications of AURA is found in Kristensen et al.[8] All instruments were placed outside the temperature-controlled room. Table 1 shows the experimental conditions for all experiments performed in this work.

The experimental setup used in these experiments is similar to Thomsen et al.,[12] except that particle samples are sampled continuously with a 3S (Aerosol Devices, series 110A), and the concentration of the precursor VOC is measured with a proton transfer reaction mass spectrometer (PTR-QMS, Ionicon Analytik) in July experiments. The 3S is run without a denuder in front with a flow rate of 1.25 L min^{-1}, a conditioner temperature of 5 °C, an initiator temperature of 35 °C, a moderator temperature of 8 °C, a nozzle temperature of 27 °C, and a sample plate temperature of 35 °C. Particle samples are collected for 15 min per well in September and October experiments and 30 min per well in July experiments. The samples are extracted in 10% acetonitrile in Milli-Q water, denoted the acid fraction, and then again in 50% acetonitrile in Milli-Q water, denoted the dimer fraction. The particle extracts are analyzed according to Thomsen et al.[12] using ultra-high-performance liquid chromatography (UHPLC) coupled to a quadrupole time-of-flight mass spectrometer (QTOF-MS, Bruker). The details of sample extraction and analysis are found in the Section S1, Supporting Information. Due to analytical issues with 3S samples from the July experiments, only data from the September and October experiments are reported. For July experiments, one particle sample is sampled onto polytetrafluoroethylene (PTFE) filters without a denuder in front of the filter holder for 30 min with a flow rate of ∼16 L min^{-1} after 6 h of experiment time. For September and October experiments, one particle sample is sampled onto PTFE filters for 15 min with a flow rate of ∼16 L min^{-1} after 6 h of experiment time. The filter samples were collected to improve the detection of low-concentration compounds such as dimers. The extraction of the filters is described elsewhere.[12] The particle extracts are analyzed both by UHPLC-QTOF-MS and by UHPLC coupled to a Q Exactive Hybrid-Quadrupole-Orbitrap mass spectrometer (Orbitrap MS, Thermo Scientific). The UHPLC method is described in Thomsen et al.,[12] and the Orbitrap MS method is described by Zhang et al.[21] and Wang et al.[39] The details of the analysis methods are found in the Section S1, Supporting Information. The data from the Orbitrap MS is processed with MzMine 2.37[40] using the ADAP Chromatogram Builder Module[41] with the same constraints as described in Zhang et al.[21] Ozonolysis products are identified using authentic standards of α-pinene ozonolysis products (*cis*-pinic acid (Aldrich), *cis*-pinonic acid (Aldrich, 98%), and diaterpenylic acid acetate (DTAA) (kindly supplied by Y. Iinuma, TROPOS, Leipzig, Germany)),[10,12] where applicable, otherwise by analyzing the compound-specific retention times (RT)[12,42−44] and mass spectral information, such as the fragmentation patterns and precursor ion, $[M - H]^-$.[12,22,23,25,45−47] All detected dimers are tentatively quantified using DTAA with a limit of detection of 11.6 ng m^{-3} as a surrogate, according to Kristensen et al.[10] Detected carboxylic acids with no authentic standard available are

https://doi.org/10.1021/acs.est.2c04786
Environ. Sci. Technol. 2022, 56, 16643−16651

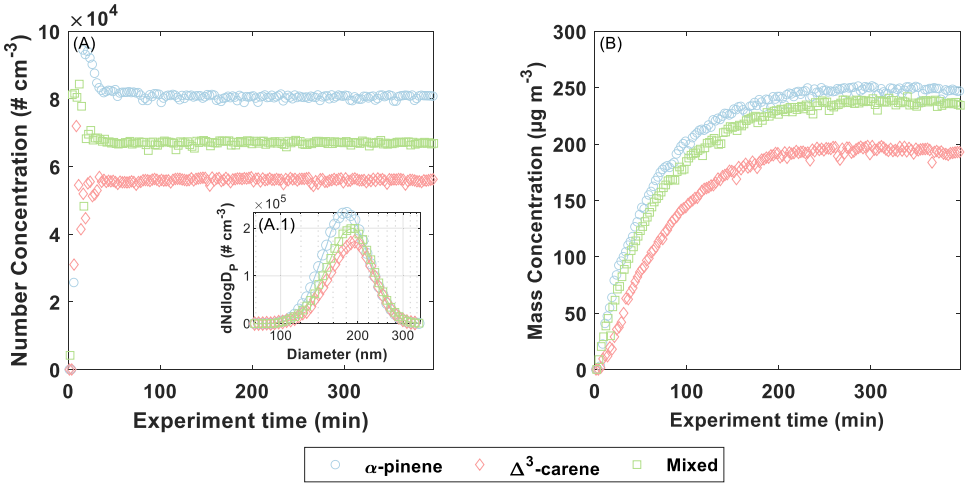

Figure 1. (A) Wall-loss corrected particle number concentrations in # cm^{-3}. (A.1) Particle size distributions at maximum particle mass concentrations. (B) Wall-loss corrected particle mass concentrations in μg m^{-3} as derived from integrated scanning mobility particle sizer (SMPS) data. The time of injection of the monoterpenes corresponds to time 0. Experiments from dates 210706, 210708, and 210713 are shown here.

tentatively quantified using a surrogate standard. The surrogate standard is determined from closeness in chemical structure and closeness in retention time.

■ RESULTS AND DISCUSSION

Experimental overviews, including the development in particle number concentration, particle mass concentration, particle mode diameter, VOC and ozone concentrations, temperature, and relative humidity, are found in Figures S2.1−2.6.

Particle Number and Mass Concentrations. Figure 1 shows the measured particle number concentrations and scanning mobility particle sizer (SMPS)-derived particle mass concentrations for the experiments from dates 210706, 210708, and 210713. Figure S3.1 shows the corresponding figure for the repeat experiments from dates 210923, 211007, and 211012. Ozonolysis of α-pinene results in a particle number concentration in the range (6.2−11.8) × 10^4 # cm^{-3} with an average of (9 ± 4) × 10^4 # cm^{-3}. Ozonolysis of Δ^3-carene results in a particle number concentration of (5.6−7.2) × 10^4 # cm^{-3} with an average of (6 ± 1) × 10^4 # cm^{-3}. Simultaneous ozonolysis of α-pinene and Δ^3-carene results in a particle number concentration in the range (6.2−8.4) × 10^4 # cm^{-3} with an average of (7 ± 2) × 10^4 # cm^{-3}. There seems to be a tendency that ozonolysis of α-pinene produces a higher particle number concentration than the ozonolysis of Δ^3-carene, in accordance with our previous study.[12] When α-pinene and Δ^3-carene are oxidized simultaneously, the resulting particle number concentration lies between the two or is comparable to the particle number concentration from ozonolysis of only α-pinene. Firm conclusions on the particle number concentrations are however not possible since there is some variation in the initial concentration of the VOCs. Ozonolysis of the individual monoterpenes as well as the simultaneous ozonolysis result in particles of approximately the same size ranging from 181 to 195 nm (Figure 1A.1) at the maximum particle mass. The particle maximum mass concentrations (after wall correction) range from 232 to 251 μg m^{-3} for ozonolysis of α-pinene, from 167 to 198 μg m^{-3} for ozonolysis of Δ^3-carene, and from 232 to 242 μg m^{-3} for simultaneous ozonolysis of α-pinene and Δ^3-carene. The particle maximum mass concentrations show that ozonolysis of α-pinene results in a higher particle mass (average of 241 ± 13 μg m^{-3}) compared to ozonolysis of Δ^3-carene (average of 181 ± 23 μg m^{-3}) and simultaneous oxidation of α-pinene and Δ^3-carene (average of 235 ± 9 μg m^{-3}), resulting in an in-between or similar particle mass. This should however be further investigated, as firm conclusions are not possible due to the variation in the initial concentration of the VOCs.

It is interesting to compare with previous observations from the AURA chamber,[12] where α-pinene and Δ^3-carene were oxidized at slightly different conditions with initial VOC concentrations of ∼50 ppb and ozone concentrations of 100−213 ppb. In the previous study, particles from ozonolysis of 50 ppb Δ^3-carene resulted in larger particles (∼180 nm) compared to particles from ozonolysis of 50 ppb α-pinene (∼120 nm) at the maximum particle mass concentration.[10,12] Ozonolysis of 50 ppb Δ^3-carene resulted in a higher particle mass than 50 ppb α-pinene.[12,13] This was speculated to arise from enhanced condensation for Δ^3-carene oxidation products because of more symmetrical product structures.[12] Figure S4.1 shows the estimated SOA yields for α-pinene and Δ^3-carene at 20 °C at different VOC loading, suggesting that at low VOC loading, the SOA yield from Δ^3-carene ozonolysis is higher than for α-pinene ozonolysis, while at higher VOC loading, the SOA yields are more similar (Figure S4.1).

The offline analysis of particle filter samples collected after 6 h shows a large contribution from 10-hydroxy-pinonic acid (OH-pinonic acid) and oxopinonic acid in the α-pinene system (Figures S5.1 and S5.2). The corresponding figures for the October experiments are shown in Figures S5.3 and S5.4. These acids are formed by reactions with OH radicals through the hydroperoxide pathway.[43,44] This indicates that the chemistry at an initial VOC concentration of α-pinene of 100 ppb is more influenced by OH radical chemistry than for an initial α-pinene concentration of 50 ppb. This shift is partly seen for ozonolysis of Δ^3-carene, where 10-hydroxy-caronic acid (OH-caronic acid) is found at a higher concentration compared to *cis*-caronic acid, but the ozonolysis product distribution is still dominated by *cis*-caric acid, as previously observed.[12] Figure S5.5 shows the product distributions for the carboxylic acids from this study, Thomsen et al.,[12] and Kristensen et al.[10] for comparison. This shift in both the SOA yield and the high increase in OH-pinonic acid and oxopinonic

https://doi.org/10.1021/acs.est.2c04786
Environ. Sci. Technol. 2022, 56, 16643−16651

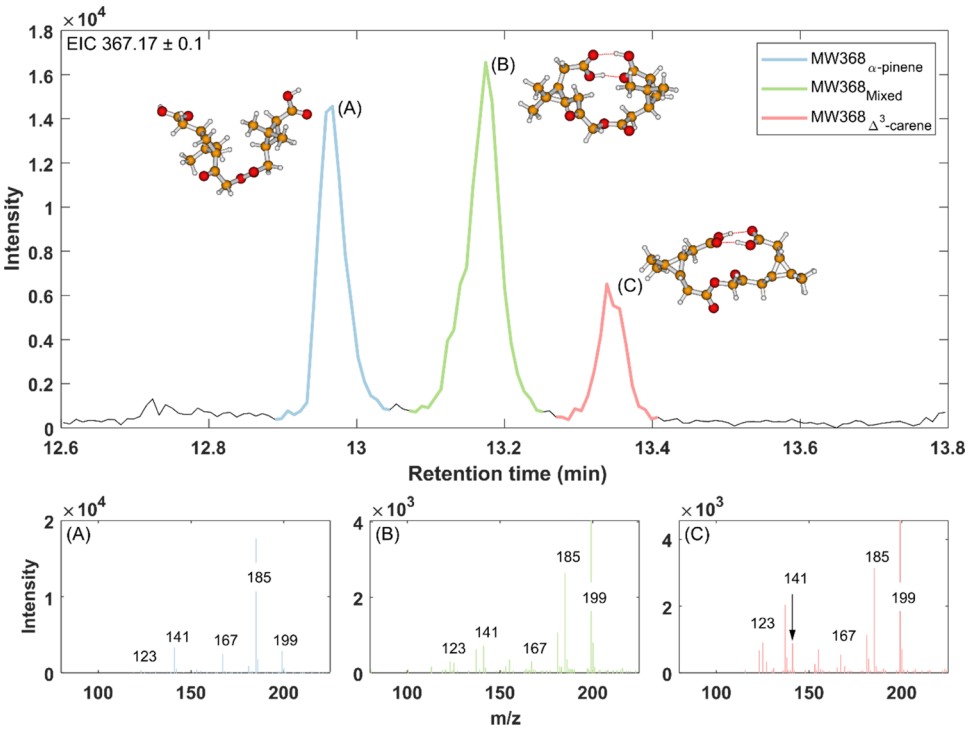

Figure 2. Chromatogram (upper panel) shows three peaks (A), (B), and (C) present in the extracted ion chromatogram (EIC) for m/z 367.17 ± 0.1, along with the possible structures of the dimers. The mass spectra (MS^2) corresponding to peaks A, B, and C are shown in the lower panels. Dimers A and C correspond to dimers tentatively identified in the α-pinene system and Δ^3-carene system, respectively. Dimer B is suggested to be a VOC-cross-product dimer composed of one *cis*-caric acid unit and one OH-pinonic acid unit. Data from analysis with QTOF-MS of a filter sample from experiment performed on date 211012.

acid indicates that OH chemistry plays a key role at the higher initial VOC concentration.

Identification of VOC-Cross-Product Dimers. Dimers are tentatively identified from their molecular ion and characteristic fragmentation patterns.[12,22,23,25,28,45−47] Figure 2 shows an extracted ion chromatogram (EIC) of m/z 367.18 corresponding to the $[M - H]^-$ of dimer MW368. Panels (A)−(C) show the mass spectra of each peak. The data is from simultaneous ozonolysis of the two monoterpenes, and the filter sample was analyzed with QTOF-MS. The chromatographic peak denoted (A) has the same RT of 12.95 min as the dimer MW368 tentatively identified from α-pinene. The chromatogram and mass spectrum (MS^2) for the MW368 dimer from α-pinene ozonolysis is shown in Figure S6.1. The peak denoted (C) has the same RT of 13.34 min as the dimer MW368 tentatively identified from Δ^3-carene. The chromatogram and mass spectrum (MS^2) for the MW368 dimer from Δ^3-carene ozonolysis is shown in Figure S6.2. The peak denoted (B) with an RT of 13.17 min is not present in particles from ozonolysis of α-pinene or Δ^3-carene individually. In all three mass spectra, the characteristic fragmentation pattern (m/z 199, 185, 167, 141, 123)[23] for MW368 is present. This suggests that VOC-cross-product dimers exist, and this is the first reported evidence of VOC-cross-product dimers. In the α-pinene system, MW368 has been suggested to consist of an ester of the monomeric units *cis*-pinic acid and OH-pinonic acid.[28,48] In the Δ^3-carene system, the MW368 is speculated to consist of the analogue monomeric units *cis*-caric acid and OH-caronic acid. In the simultaneous ozonolysis of α-pinene and Δ^3-carene, both *cis*-pinic acid, *cis*-caric acid, OH-pinonic acid, and OH-caronic acid are present. We suggest that the MW368 dimer only observed in the mixed system is a VOC-cross-product dimer ester consisting of one α-pinene constituent and one Δ^3-carene constituent. The most likely conformation is one *cis*-caric acid unit and one OH-pinonic acid unit as the concentration of *cis*-caric acid exceeds that of *cis*-pinic acid, and the concentration of OH-pinonic acid exceeds that of OH-caronic acid (Figures S5.1 and S5.2). The VOC-cross-product dimer is also observed in particles collected with the 3S (Figure S5.3, exp. 211012).

Quantum chemical calculations reveal that the lowest free energy structures of the proposed carene MW368 and the mixed MW368 dimer esters have two carboxylic acid moieties forming intramolecular hydrogen bonds (Figures 2 and S7.1). This is not the case for the MW368 pinic dimer ester. These differences may influence the observed UHPLC retention times. A detailed description of the quantum chemical calculations is found in Figure S7.1. In addition to the MW368 VOC-cross-product dimer, a VOC-cross-product dimer for MW338 is also identified. The chromatograms and mass spectra (MS^2) for the dimer tentatively identified in all three ozonolysis systems are presented in Figures S6.4−S6.6. The MW338 dimer ester is suggested to be the ester of a caronaldehyde or pinonaldehyde unit and a terpenylic acid unit. Terpenylic acid is observed both in the ozonolysis of α-pinene and Δ^3-carene individually (Figures S5.1 and S5.2), but the concentration of terpenylic acid in the α-pinene ozonolysis exceeds that of the terpenylic acid concentration from Δ^3-carene ozonolysis. Therefore, the most likely structure of the mixed MW338 dimer is composed of a terpenylic acid unit (from α-pinene ozonolysis) and a caronaldehyde unit.

Particle Product Distributions. Figure 3 shows the development over time of the total concentration of carboxylic acids, the SMPS particle mass concentration, and the

https://doi.org/10.1021/acs.est.2c04786
Environ. Sci. Technol. 2022, 56, 16643−16651

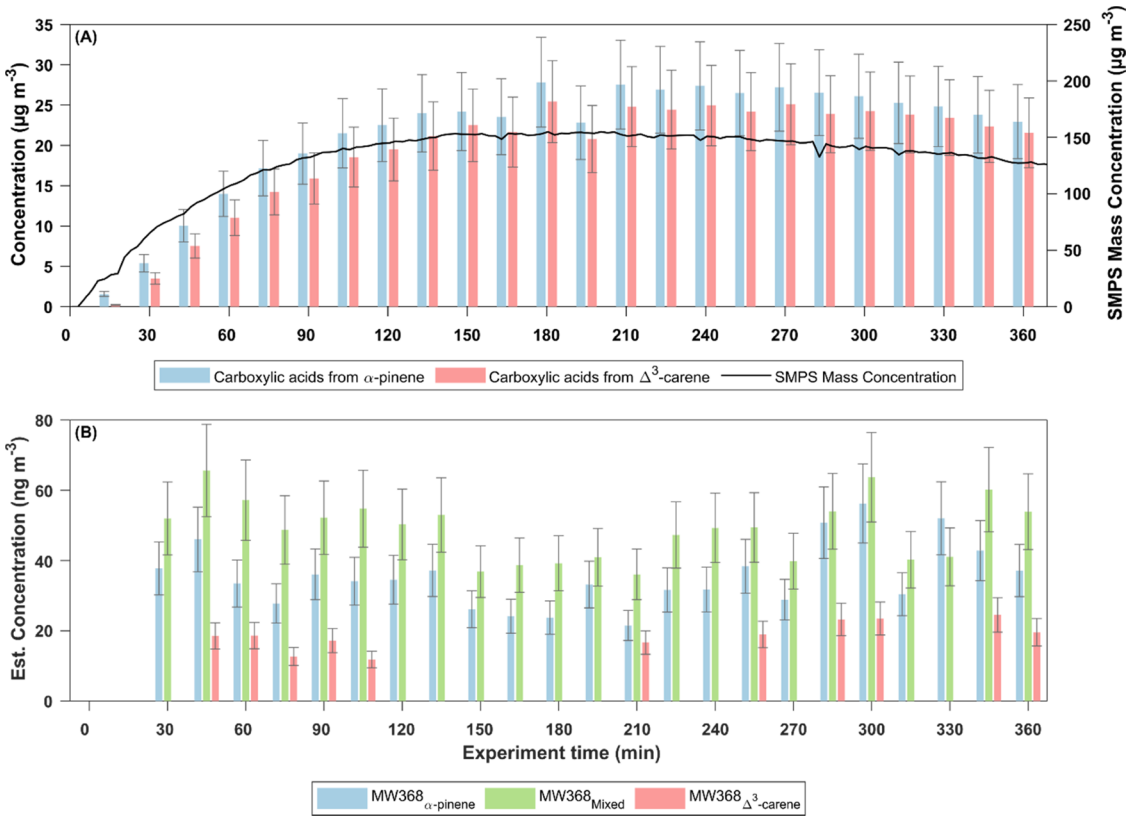

Figure 3. Time-resolved concentrations of oxidation products in SOA from ozonolysis of a mix of α-pinene and Δ^3-carene. (A) Evolution of the total carboxylic acid concentration in μg m^{-3} with an estimated uncertainty of ±20% and the evolution in the SMPS particle mass concentration (black line). Note that the scales on the two *y*-axes are different. (B) Evolution of dimer MW368 from α-pinene, dimer MW368 from Δ^3-carene, and the VOC-cross-product dimer, MW368, in ng m^{-3} with an estimated uncertainty of ±20%. The particles are sampled with 3S, and the analysis is performed with QTOF-MS. Data is from the experiment performed on date 211012.

development over time in the concentration of all three MW368 dimers, which were tentatively identified in the targeted filter analysis of the mixed ozonolysis system (Figure 2). The trend in the total carboxylic acid concentration is very similar to the particle mass concentration derived from an SMPS (Figure 1B). The concentration of carboxylic acids from ozonolysis of α-pinene exceeds that of carboxylic acids from ozonolysis of Δ^3-carene already after 15 min, which is consistent with the development in the particle mass concentration. We find that *cis*-caric acid is detected already after 15 min, whereas *cis*-pinic acid is only detected after 30 min (Figure S8.2A). This indicates that *cis*-caric acid has the potential to condense earlier than *cis*-pinic acid, either because the concentration of *cis*-caric acid in the gas phase is higher than the *cis*-pinic acid gas-phase concentration or because the condensation of *cis*-caric acid is more favorable than the condensation of *cis*-pinic acid in line with previous research.[12] After about 210 min, the total concentration of carboxylic acids decreases, which is consistent with the time evolution in the particle mass concentration, where the wall loss exceeds the production of particle mass toward the end of the experiment. The wall loss is not identical for all products, e.g., *cis*-caric acid and *cis*-pinic acid do not show this decrease (Figure S8.2A), but OH-pinonic acid and OH-caronic acid do show a decrease in concentration (Figure S8.2B). It has previously been suggested that wall loss of semi-volatiles is proportional to their vapor pressures.[49] The estimated vapor pressures of the OH-pinonic acid and OH-caronic acid are higher than that of *cis*-caric acid and *cis*-pinic acid,[12] which might explain the differences in wall loss for the products. Another potential explanation for the differences in the wall loss of the products could be that OH-pinonic acid and OH-caronic acid may undergo further particle-phase reactions and thereby decrease in concentration.

Figure 3B shows the estimated concentrations of the MW368 dimers with time. The contribution from the Δ^3-carene dimer is lower than the corresponding α-pinene dimer, in agreement with previous observations.[12] The concentration of the Δ^3-carene MW368 dimer fluctuates around the detection limit and is thus not detected in all sampling wells. The concentration of dimers seems relatively constant over time and does not follow the evolution of the total carboxylic acids nor the particle mass concentration. This is in line with previous work, suggesting that dimers form early in the experiment and condense almost immediately, making their levels in the particle phase constant in contrast to carboxylic acids.[22,23] Formation of dimers thus seems to be linked to the presence of high levels of gas-phase radicals such as peroxy radicals and Criegee intermediates rather than the concentration of carboxylic acids in the particle phase, indicating that dimers are formed in the gas phase or by heterogeneous reactions rather than by bulk particle-phase reactions.

Figures S5.1 and S5.2 show the carboxylic acid fraction, while Figures S5.3 and S5.4 show the dimer fraction of the targeted analysis in particle filter samples performed on an Orbitrap MS. The α-pinene ozonolysis product distribution is diverse, and 12 carboxylic acids and 23 dimers have been tentatively identified. The Δ^3-carene product distribution is

https://doi.org/10.1021/acs.est.2c04786
Environ. Sci. Technol. 2022, 56, 16643−16651

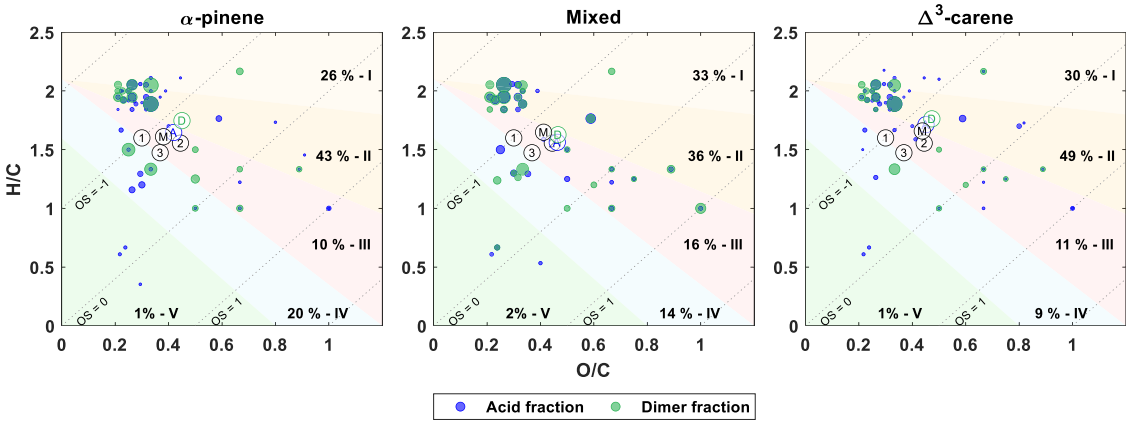

Figure 4. MCR-VK diagrams for ozonolysis of α-pinene, Δ^3-carene, and the mixed system. The blue dots are compounds detected in the carboxylic acid fraction. The green dots are compounds detected in the dimer fraction. For both groups, the size of the dot is the normalized intensity measured by Orbitrap MS. A is the average O/C and H/C ratio from the acid fraction, D is the average OC/HC ratio from the dimer fraction, M is the average OC/HC ratio from the AMS, 1 is the OC/HC ratio for *cis*-pinonic acid or *cis*-caronic acid, 2 is the OC/HC ratio for *cis*-pinic acid or *cis*-caric acid, and 3 is the OC/HC ratio for the dimer MW368. The Roman numbers refer to the MCR classification, where I: very highly oxidized, II: highly oxidized, III: intermediately oxidized, IV: oxidized unsaturated, and V: highly unsaturated.[22] Data is from experiments performed on dates 210706, 210708, and 210713. Particles were sampled on a filter and analyzed using Orbitrap MS.

simple, with a major contribution from *cis*-caric acid and minor contributions from three other carboxylic acids. A total of seven dimers have been tentatively identified for the individual ozonolysis of Δ^3-carene. In our previous work, only three dimers (MW338, MW368, and MW400) were tentatively identified from Δ^3-carene.[12] Here, Δ^3-carene analogues of the known α-pinene dimers MW342, MW344a, MW356, and MW386 have also been tentatively identified by their fragmentation patterns. Table S9.1 shows the compounds' m/z ratios and their characteristic fragmentation patterns. The observation that ozonolysis of α-pinene results in a diverse product distribution and the ozonolysis of Δ^3-carene results in a simpler product distribution is in line with previous work.[8,10,12] Simultaneous ozonolysis of α-pinene and Δ^3-carene results in a product distribution for the carboxylic acids, which appears like the combination of the product distributions in SOA from separate ozonolysis of α-pinene and Δ^3-carene, respectively. The dimer product distribution from ozonolysis of their mixture is similar, except that contributions from some α-pinene dimers (MW302, MW316, MW356, MW384, and MW400) are missing. Of these, the molecular structures of the dimers MW302, M316, MW400, and MW384 are unknown. The dimer ester MW356 is suggested to consist of a *cis*-caric acid unit and a terpenylic acid unit. It remains unclear why these dimers do not form in the mixed system. In addition to the dimers tentatively identified in the individual analysis, mixed dimers of MW368 and MW338 are tentatively identified.

Targeted analysis identifies and quantifies about 15−30% of the composition of laboratory-generated monoterpene SOA collected at 20 °C,[8,12] but the remaining unidentified percentage of the particle fraction is equally important in estimating the effects of aerosols on both climate and human health.[21] As the unknown fraction is difficult to interpret, different visual tools such as the van Krevelen plot combined with the maximum carbonyl ratio (MCR-VK) are applied.[21] MCR-VK plots are divided into five categories, with category I describing very highly oxidized species, e.g., isoprene oxidation products or peroxides, category II describing highly oxidized species, e.g., monoterpene oxidation products and oxidative aging products, category III describing intermediately oxidized species, e.g., first-generation monoterpene oxidation products, category IV describing oxidized unsaturated compounds, e.g., primary organic carbon, and category V describing highly unsaturated compounds, e.g., combustion-related and condensational aging species. Compounds fall into a category depending on their H/C ratio and O/C ratio. Figure 4 shows the MCR-VK plots from the nontargeted analysis of particles collected onto filters. Overall, the MCR-VK plots are similar for the ozonolysis of α-pinene and Δ^3-carene individually. The majority of products lie in category II and fall into the category of highly oxidized compounds. Compounds typically found in this category include monoterpene oxidation products, oxidative aging products, and higher-generation oxidation products. These products include both biogenic, biomass burning, and anthropogenic compounds, e.g., 3-methyl-1,2,3-butanetricarboxylic acid from α-pinene oxidation, highly oxygenated organic molecules (HOMs), levoglucosan from biomass burning, and adipic acid from anthropogenic activities.[21] This is also seen for the simultaneous ozonolysis; however, during this experiment, the degree of oxidation is influenced by more intermediately oxidized products in groups III and IV. Intermediately oxidized products include first-generation monoterpene oxidation products, e.g., *cis*-pinic acid and *cis*-caric acid.[21] In all three systems, about one-third of the products fall into category I, which is very highly oxidized. Category I usually includes isoprene oxidation products or oxidation products of small VOCs.[21] Previous observations from flow tube experiments of ozonolysis of α-pinene show that the majority of products are found in III and IV.[21] The large contribution to group I in this work is speculated to arise from highly oxygenated organic molecules with peroxide functionalities. Figure S10.1 presents the MCR-VK diagram for the July experiments. The differences between the systems are not as pronounced for this set of experiments. The largest difference is the fraction found in category I. In Figure S10.1, ∼15% is found in category I compared to the ∼33% in Figure 4. The loss of the very highly oxidized products may arise from the difference in the sampling time (30 vs 15 min) or in the storage time (∼3 or ∼1 month), as peroxides will easily react

https://doi.org/10.1021/acs.est.2c04786
Environ. Sci. Technol. 2022, 56, 16643−16651

or decompose. The nontargeted analysis of both the acid fraction and the dimer fraction results in an average O/C and H/C, which is very comparable to the average O/C and H/C measured by a high-resolution time-of-flight aerosol mass spectrometer (AMS).

Atmospheric Implications. The formation of SOA from biogenic compounds is important to understand as it is a complicated mechanism influenced by numerous factors. Formation of SOA from complex and nonideal mixing of monoterpenes can result in an enhancement in particle mass compared to oxidation of monoterpenes individually,[18,19] while influence from other BVOCs such as isoprene leads to decreases in the SOA yield.[20] In this work, we find that a mixture of the two structurally alike monoterpenes α-pinene and Δ^3-carene results in a particle mass concentration that is lower or similar to the one from the individual ozonolysis of α-pinene. From the mixture of the two structurally similar monoterpenes, no mass enhancement or decrease is observed in contrast to previous work with mixtures of VOCs. Previous work shows that ozonolysis of Δ^3-carene produced a higher particle mass concentration in comparison with the ozonolysis of α-pinene. A shift in the particle product distribution is observed, and the discrepancy is likely caused by a shift in the chemical mechanism from being ozone-dominated to being more influenced by OH radicals. This indicates that the VOC loading is important for relative yields of products upon ozonolysis. The influence of the VOC loading on the resulting SOA yield and product distributions should be subject to further research. Another important finding is the evidence of VOC-cross-product dimers. Until now, no VOC-cross-product dimers have been detected experimentally. The existence of VOC-cross-product dimers implies that dimers at ambient conditions might consist of subunits from different terpene precursors, in line with previous suggestions that pure α-pinene accretion products compete with cross-reactions.[50] This will lead to a more complex distribution of dimers in the atmosphere, which might influence new particle formation.

■ ASSOCIATED CONTENT

Supporting Information

The Supporting Information is available free of charge at https://pubs.acs.org/doi/10.1021/acs.est.2c04786.

> Experimental overviews, particle number concentration, and particle mass concentration for October experiments, the relationship between initial VOC loading and particle mass concentration, targeted analysis, proof of cross-product dimers, time evolution of important oxidation products, maximum carbonyl-van Krevelen plot for July experiments, identification of dimers from Δ^3-carene, description of quantum chemical calculation of possible dimer structures (PDF)

■ AUTHOR INFORMATION

Corresponding Author

Marianne Glasius − *Department of Chemistry, Aarhus University, DK-8000 Aarhus C, Denmark;* orcid.org/0000-0002-4404-6989; Email: glasius@chem.au.dk

Authors

Ditte Thomsen − *Department of Chemistry, Aarhus University, DK-8000 Aarhus C, Denmark;* orcid.org/0000-0002-3110-8503

Lotte Dyrholm Thomsen − *Department of Chemistry, Aarhus University, DK-8000 Aarhus C, Denmark*

Emil Mark Iversen − *Department of Chemistry, Aarhus University, DK-8000 Aarhus C, Denmark;* orcid.org/0000-0002-6344-3939

Thurídur Nótt Björgvinsdóttir − *Department of Chemistry, Aarhus University, DK-8000 Aarhus C, Denmark*

Sofie Falk Vinther − *Department of Chemistry, Aarhus University, DK-8000 Aarhus C, Denmark*

Jane Tygesen Skønager − *Department of Chemistry, Aarhus University, DK-8000 Aarhus C, Denmark*

Thorsten Hoffmann − *Department of Chemistry, Johannes Gutenberg University, 55128 Mainz, Germany*

Jonas Elm − *Department of Chemistry, Aarhus University, DK-8000 Aarhus C, Denmark;* orcid.org/0000-0003-3736-4329

Merete Bilde − *Department of Chemistry, Aarhus University, DK-8000 Aarhus C, Denmark;* orcid.org/0000-0002-2112-514X

Complete contact information is available at: https://pubs.acs.org/10.1021/acs.est.2c04786

Author Contributions

The manuscript was written through contributions of all authors. All authors have given approval to the final version of the manuscript.

Notes

The authors declare no competing financial interest.

■ ACKNOWLEDGMENTS

The authors thank the Independent Research Fund Denmark, the Carlsberg Foundation, and Aarhus University for financial support. The authors thank laboratory manager Mads Mørk Jensen for his assistance in the laboratory. The authors thank Anders Feilberg and Kasper Kristensen for providing a PTR-QMS. D.T. thanks Anja Beschnitt and Regina Huesmann for introducing her to and assisting her in the Hoffman Laboratory.

■ REFERENCES

(1) Hallquist, M.; Wenger, J. C.; Baltensperger, U.; Rudich, Y.; Simpson, D.; Claeys, M.; Dommen, J.; Donahue, N. M.; George, C.; Goldstein, A. H.; Hamilton, J. F.; Herrmann, H.; Hoffmann, T.; Iinuma, Y.; Jang, M.; Jenkin, M. E.; Jimenez, J. L.; Kiendler-Scharr, A.; Maenhaut, W.; McFiggans, G.; Mentel, T. F.; Monod, A.; Prévôt, A. S. H.; Seinfeld, J. H.; Surratt, J. D.; Szmigielski, R.; Wildt, J. The formation, properties and impact of secondary organic aerosol: current and emerging issues. *Atmos. Chem. Phys.* **2009**, *9*, 5155−5236.

(2) IPCC. *Climate Change 2013: The Physical Science Basis. Contribution of Working Group I to the Fifth Assessment Report of the Intergovernmental Panel on Climate Change*; Cambridge University Press, 2013.

(3) Kim, K.-H.; Kabir, E.; Kabir, S. A review on the human health impact of airborne particulate matter. *Environ. Int.* **2015**, *74*, 136−143.

(4) Shiraiwa, M.; Ueda, K.; Pozzer, A.; Lammel, G.; Kampf, C. J.; Fushimi, A.; Enami, S.; Arangio, A. M.; Fröhlich-Nowoisky, J.; Fujitani, Y.; Furuyama, A.; Lakey, P. S. J.; Lelieveld, J.; Lucas, K.; Morino, Y.; Pöschl, U.; Takahama, S.; Takami, A.; Tong, H.; Weber, B.; Yoshino, A.; Sato, K. Aerosol Health Effects from Molecular to Global Scales. *Environ. Sci. Technol.* **2017**, *51*, 13545−13567.

(5) Hoffmann, T.; Odum, J. R.; Bowman, F.; Collins, D.; Klockow, D.; Flagan, R. C.; Seinfeld, J. H. Formation of Organic Aerosols from

the Oxidation of Biogenic Hydrocarbons. *J. Atmos. Chem.* **1997**, *26*, 189−222.

(6) Pathak, R. K.; Stanier, C. O.; Donahue, N. M.; Pandis, S. N. Ozonolysis of α-pinene at atmospherically relevant concentrations: Temperature dependence of aerosol mass fractions (yields). *J. Geophys. Res.: Atmos.* **2007**, *112*, No. D03201.

(7) Laj, P.; Klausen, J.; Bilde, M.; Plaß-Duelmer, C.; Pappalardo, G.; Clerbaux, C.; Baltensperger, U.; Hjorth, J.; Simpson, D.; Reimann, S.; Coheur, P. F.; Richter, A.; De Mazière, M.; Rudich, Y.; McFiggans, G.; Torseth, K.; Wiedensohler, A.; Morin, S.; Schulz, M.; Allan, J. D.; Attié, J. L.; Barnes, I.; Birmili, W.; Cammas, J. P.; Dommen, J.; Dorn, H. P.; Fowler, D.; Fuzzi, S.; Glasius, M.; Granier, C.; Hermann, M.; Isaksen, I. S. A.; Kinne, S.; Koren, I.; Madonna, F.; Maione, M.; Massling, A.; Moehler, O.; Mona, L.; Monks, P. S.; Müller, D.; Müller, T.; Orphal, J.; Peuch, V. H.; Stratmann, F.; Tanré, D.; Tyndall, G.; Abo Riziq, A.; Van Roozendael, M.; Villani, P.; Wehner, B.; Wex, H.; Zardini, A. A. Measuring atmospheric composition change. *Atmos. Environ.* **2009**, *43*, 5351−5414.

(8) Kristensen, K.; Jensen, L. N.; Glasius, M.; Bilde, M. The effect of sub-zero temperature on the formation and composition of secondary organic aerosol from ozonolysis of alpha-pinene. *Environ. Sci.: Processes Impacts* **2017**, *19*, 1220−1234.

(9) Quéléver, L. L. J.; Kristensen, K.; Normann Jensen, L.; Rosati, B.; Teiwes, R.; Daellenbach, K. R.; Peräkylä, O.; Roldin, P.; Bossi, R.; Pedersen, H. B.; Glasius, M.; Bilde, M.; Ehn, M. Effect of temperature on the formation of highly oxygenated organic molecules (HOMs) from alpha-pinene ozonolysis. *Atmos. Chem. Phys.* **2019**, *19*, 7609−7625.

(10) Kristensen, K.; Jensen, L. N.; Quéléver, L. L. J.; Christiansen, S.; Rosati, B.; Elm, J.; Teiwes, R.; Pedersen, H. B.; Glasius, M.; Ehn, M.; Bilde, M. The Aarhus Chamber Campaign on Highly Oxidized Multifunctional Organic Molecules and Aerosols (ACCHA): Particle Formation and Detailed Chemical Composition at Different Temperatures. *Atmos. Chem. Phys.* **2020**, *20*, 12549−12567.

(11) Simon, M.; Dada, L.; Heinritzi, M.; Scholz, W.; Stolzenburg, D.; Fischer, L.; Wagner, A. C.; Kürten, A.; Rörup, B.; He, X.-C.; Almeida, J.; Baalbaki, R.; Baccarini, A.; Bauer, P. S.; Beck, L.; Bergen, A.; Bianchi, F.; Bräkling, S.; Brilke, S.; Caudillo, L.; Chen, D.; Chu, B.; Dias, A.; Draper, D. C.; Duplissy, J.; El Haddad, I.; Finkenzeller, H.; Frege, C.; Gonzalez-Carracedo, L.; Gordon, H.; Granzin, M.; Hakala, J.; Hofbauer, V.; Hoyle, C. R.; Kim, C.; Kong, W.; Lamkaddam, H.; Lee, C. P.; Lehtipalo, K.; Leiminger, M.; Mai, H.; Manninen, H. E.; Marie, G.; Marten, R.; Mentler, B.; Molteni, U.; Nichman, L.; Nie, W.; Ojdanic, A.; Onnela, A.; Partoll, E.; Petäjä, T.; Pfeifer, J.; Philippov, M.; Quéléver, L. L. J.; Ranjithkumar, A.; Rissanen, M.; Schallhart, S.; Schobesberger, S.; Schuchmann, S.; Shen, J.; Sipilä, M.; Steiner, G.; Stozhkov, Y.; Tauber, C.; Tham, Y. J.; Tomé, A. R.; Vazquez-Pufleau, M.; Vogel, A.; Wagner, R.; Wang, M.; Wang, D. S.; Wang, Y.; Weber, S. K.; Wu, Y.; Xiao, M.; Yan, C.; Ye, P.; Ye, Q.; Zauner-Wieczorek, M.; Zhou, X.; Baltensperger, U.; Dommen, J.; Flagan, R. C.; Hansel, A.; Kulmala, M.; Volkamer, R.; Winkler, P. M.; Worsnop, D. R.; Donahue, N. M.; Kirkby, J.; Curtius, J. Molecular understanding of new-particle formation from alpha-pinene between -50 and +25 °C. *Atmos. Chem. Phys.* **2020**, *20*, 9183−9207.

(12) Thomsen, D.; Elm, J.; Rosati, B.; Skønager, J. T.; Bilde, M.; Glasius, M. Large Discrepancy in the Formation of Secondary Organic Aerosols from Structurally Similar Monoterpenes. *ACS Earth Space Chem.* **2021**, *5*, 632−644.

(13) Jonsson, Å. M.; Hallquist, M.; Ljungström, E. The effect of temperature and water on secondary organic aerosol formation from ozonolysis of limonene, Δ3-carene and α-pinene. *Atmos. Chem. Phys.* **2008**, *8*, 6541−6549.

(14) Ehn, M.; Thornton, J. A.; Kleist, E.; Sipilä, M.; Junninen, H.; Pullinen, I.; Springer, M.; Rubach, F.; Tillmann, R.; Lee, B.; Lopez-Hilfiker, F.; Andres, S.; Acir, I.-H.; Rissanen, M.; Jokinen, T.; Schobesberger, S.; Kangasluoma, J.; Kontkanen, J.; Nieminen, T.; Kurtén, T.; Nielsen, L. B.; Jørgensen, S.; Kjaergaard, H. G.; Canagaratna, M.; Maso, M. D.; Berndt, T.; Petäjä, T.; Wahner, A.; Kerminen, V.-M.; Kulmala, M.; Worsnop, D. R.; Wildt, J.; Mentel, T. F. A large source of low-volatility secondary organic aerosol. *Nature* **2014**, *506*, 476−479.

(15) Hoffmann, T.; Bandur, R.; Marggraf, U.; Linscheid, M. Molecular composition of organic aerosols formed in the α-pinene/O3reaction: Implications for new particle formation processes. *J. Geophys. Res.: Atmos.* **1998**, *103*, 25569−25578.

(16) Boy, M.; Mogensen, D.; Smolander, S.; Zhou, L.; Nieminen, T.; Paasonen, P.; Plass-Dülmer, C.; Sipilä, M.; Petäjä, T.; Mauldin, L.; Berresheim, H.; Kulmala, M. Oxidation of SO2 by stabilized Criegee intermediate (sCI) radicals as a crucial source for atmospheric sulfuric acid concentrations. *Atmos. Chem. Phys.* **2013**, *13*, 3865−3879.

(17) D'Ambro, E. L.; Hyttinen, N.; Møller, K. H.; Iyer, S.; Otkjær, R. V.; Bell, D. M.; Liu, J.; Lopez-Hilfiker, F. D.; Schobesberger, S.; Shilling, J. E.; Zelenyuk, A.; Kjaergaard, H. G.; Thornton, J. A.; Kurtén, T. Pathways to Highly Oxidized Products in the Δ3-Carene + OH System. *Environ. Sci. Technol.* **2022**, *56*, 2213−2224.

(18) Ahlberg, E.; Falk, J.; Eriksson, A.; Holst, T.; Brune, W. H.; Kristensson, A.; Roldin, P.; Svenningsson, B. Secondary organic aerosol from VOC mixtures in an oxidation flow reactor. *Atmos. Environ.* **2017**, *161*, 210−220.

(19) Faiola, C. L.; Buchholz, A.; Kari, E.; Yli-Pirilä, P.; Holopainen, J. K.; Kivimäenpää, M.; Miettinen, P.; Worsnop, D. R.; Lehtinen, K. E. J.; Guenther, A. B.; Virtanen, A. Terpene Composition Complexity Controls Secondary Organic Aerosol Yields from Scots Pine Volatile Emissions. *Sci. Rep.* **2018**, *8*, No. 3053.

(20) McFiggans, G.; Mentel, T. F.; Wildt, J.; Pullinen, I.; Kang, S.; Kleist, E.; Schmitt, S.; Springer, M.; Tillmann, R.; Wu, C.; Zhao, D.; Hallquist, M.; Faxon, C.; Le Breton, M.; Hallquist, Å. M.; Simpson, D.; Bergström, R.; Jenkin, M. E.; Ehn, M.; Thornton, J. A.; Alfarra, M. R.; Bannan, T. J.; Percival, C. J.; Priestley, M.; Topping, D.; Kiendler-Scharr, A. Secondary organic aerosol reduced by mixture of atmospheric vapours. *Nature* **2019**, *565*, 587−593.

(21) Zhang, Y.; Wang, K.; Tong, H.; Huang, R.-J.; Hoffmann, T. The maximum carbonyl ratio (MCR) as a new index for the structural classification of secondary organic aerosol components. *Rapid Commun. Mass Spectrom.* **2021**, *35*, No. e9113.

(22) Kristensen, K.; Cui, T.; Zhang, H.; Gold, A.; Glasius, M.; Surratt, J. D. Dimers in α-pinene secondary organic aerosol: effect of hydroxyl radical, ozone, relative humidity and aerosol acidity. *Atmos. Chem. Phys.* **2014**, *14*, 4201−4218.

(23) Kristensen, K.; Watne, Å. K.; Hammes, J.; Lutz, A.; Petäjä, T.; Hallquist, M.; Bilde, M.; Glasius, M. High-Molecular Weight Dimer Esters Are Major Products in Aerosols from α-Pinene Ozonolysis and the Boreal Forest. *Environ. Sci. Technol. Lett.* **2016**, *3*, 280−285.

(24) Lehtipalo, K.; Yan, C.; Dada, L.; Bianchi, F.; Xiao, M.; Wagner, R.; Stolzenburg, D.; Ahonen, L. R.; Amorim, A.; Baccarini, A.; Bauer, P. S.; Baumgartner, B.; Bergen, A.; Bernhammer, A.-K.; Breitenlechner, M.; Brilke, S.; Buchholz, A.; Mazon, S. B.; Chen, D.; Chen, X.; Dias, A.; Dommen, J.; Draper, D. C.; Duplissy, J.; Ehn, M.; Finkenzeller, H.; Fischer, L.; Frege, C.; Fuchs, C.; Garmash, O.; Gordon, H.; Hakala, J.; He, X.; Heikkinen, L.; Heinritzi, M.; Helm, J. C.; Hofbauer, V.; Hoyle, C. R.; Jokinen, T.; Kangasluoma, J.; Kerminen, V.-M.; Kim, C.; Kirkby, J.; Kontkanen, J.; Kürten, A.; Lawler, M. J.; Mai, H.; Mathot, S.; Mauldin, R. L.; Molteni, U.; Nichman, L.; Nie, W.; Nieminen, T.; Ojdanic, A.; Onnela, A.; Passananti, M.; Petäjä, T.; Piel, F.; Pospisilova, V.; Quéléver, L. L. J.; Rissanen, M. P.; Rose, C.; Sarnela, N.; Schallhart, S.; Schuchmann, S.; Sengupta, K.; Simon, M.; Sipilä, M.; Tauber, C.; Tomé, A.; Tröstl, J.; Väisänen, O.; Vogel, A. L.; Volkamer, R.; Wagner, A. C.; Wang, M.; Weitz, L.; Wimmer, D.; Ye, P.; Ylisirniö, A.; Zha, Q.; Carslaw, K. S.; Curtius, J.; Donahue, N. M.; Flagan, R. C.; Hansel, A.; Riipinen, I.; Virtanen, A.; Winkler, P. M.; Baltensperger, U.; Kulmala, M.; Worsnop, D. R. Multicomponent new particle formation from sulfuric acid, ammonia, and biogenic vapors. *Sci. Adv.* **2018**, *4*, No. eaau5363.

(25) Mohr, C.; Lopez-Hilfiker, F. D.; Yli-Juuti, T.; Heitto, A.; Lutz, A.; Hallquist, M.; D'Ambro, E. L.; Rissanen, M. P.; Hao, L.; Schobesberger, S.; Kulmala, M.; Mauldin, R. L.; Makkonen, U.; Sipilä, M.; Petäjä, T.; Thornton, J. A. Ambient observations of dimers from

terpene oxidation in the gas phase: Implications for new particle formation and growth. *Geophys. Res. Lett.* **2017**, *44*, 2958−2966.
(26) Hamilton, J. F.; Lewis, A. C.; Reynolds, J. C.; Carpenter, L. J.; Lubben, A. Investigating the composition of organic aerosol resulting from cyclohexene ozonolysis: low molecular weight and heterogeneous reaction products. *Atmos. Chem. Phys.* **2006**, *6*, 4973−4984.
(27) Müller, L.; Reinnig, M. C.; Warnke, J.; Hoffmann, T. Unambiguous identification of esters as oligomers in secondary organic aerosol formed from cyclohexene and cyclohexene/α-pinene ozonolysis. *Atmos. Chem. Phys.* **2008**, *8*, 1423−1433.
(28) Yasmeen, F.; Vermeylen, R.; Szmigielski, R.; Iinuma, Y.; Böge, O.; Herrmann, H.; Maenhaut, W.; Claeys, M. Terpenylic acid and related compounds: precursors for dimers in secondary organic aerosol from the ozonolysis of α- and β-pinene. *Atmos. Chem. Phys.* **2010**, *10*, 9383−9392.
(29) Tolocka, M. P.; Jang, M.; Ginter, J. M.; Cox, F. J.; Kamens, R. M.; Johnston, M. V. Formation of Oligomers in Secondary Organic Aerosol. *Environ. Sci. Technol.* **2004**, *38*, 1428−1434.
(30) Gao, S.; Ng, N. L.; Keywood, M.; Varutbangkul, V.; Bahreini, R.; Nenes, A.; He, J.; Yoo, K. Y.; Beauchamp, J. L.; Hodyss, R. P.; Flagan, R. C.; Seinfeld, J. H. Particle Phase Acidity and Oligomer Formation in Secondary Organic Aerosol. *Environ. Sci. Technol.* **2004**, *38*, 6582−6589.
(31) Hasan, G.; Salo, V.-T.; Valiev, R. R.; Kubečka, J.; Kurtén, T. Comparing Reaction Routes for 3(RO···OR′) Intermediates Formed in Peroxy Radical Self- and Cross-Reactions. *J. Phys. Chem. A* **2020**, *124*, 8305−8320.
(32) Salo, V.-T.; Valiev, R.; Lehtola, S.; Kurtén, T. Gas-Phase Peroxyl Radical Recombination Reactions: A Computational Study of Formation and Decomposition of Tetroxides. *J. Phys. Chem. A* **2022**, *126*, 4046−4056.
(33) Turpin, B. J.; Saxena, P.; Andrews, E. Measuring and simulating particulate organics in the atmosphere: problems and prospects. *Atmos. Environ.* **2000**, *34*, 2983−3013.
(34) Vecchi, R.; Valli, G.; Fermo, P.; D'Alessandro, A.; Piazzalunga, A.; Bernardoni, V. Organic and inorganic sampling artefacts assessment. *Atmos. Environ.* **2009**, *43*, 1713−1720.
(35) Eiguren-Fernandez, A.; Lewis, G. S.; Spielman, S. R.; Hering, S. V. Time-resolved characterization of particle associated polycyclic aromatic hydrocarbons using a newly-developed sequential spot sampler with automated extraction and analysis. *Atmos. Environ.* **2014**, *96*, 125−134.
(36) Hering, S. V.; Spielman, S. R.; Lewis, G. S. Moderated, Water-Based, Condensational Particle Growth in a Laminar Flow. *Aerosol Sci. Technol.* **2014**, *48*, 401−408.
(37) Tu, P.; Johnston, M. V. Particle size dependence of biogenic secondary organic aerosol molecular composition. *Atmos. Chem. Phys.* **2017**, *17*, 7593−7603.
(38) Zhao, Z.; Tolentino, R.; Lee, J.; Vuong, A.; Yang, X.; Zhang, H. Interfacial Dimerization by Organic Radical Reactions during Heterogeneous Oxidative Aging of Oxygenated Organic Aerosols. *J. Phys. Chem. A* **2019**, *123*, 10782−10792.
(39) Wang, K.; Zhang, Y.; Huang, R.-J.; Cao, J.; Hoffmann, T. UHPLC-Orbitrap mass spectrometric characterization of organic aerosol from a central European city (Mainz, Germany) and a Chinese megacity (Beijing). *Atmos. Environ.* **2018**, *189*, 22−29.
(40) Pluskal, T.; Castillo, S.; Villar-Briones, A.; Orešič, M. MZmine 2: Modular framework for processing, visualizing, and analyzing mass spectrometry-based molecular profile data. *BMC Bioinf.* **2010**, *11*, No. 395.
(41) Myers, O. D.; Sumner, S. J.; Li, S.; Barnes, S.; Du, X. One Step Forward for Reducing False Positive and False Negative Compound Identifications from Mass Spectrometry Metabolomics Data: New Algorithms for Constructing Extracted Ion Chromatograms and Detecting Chromatographic Peaks. *Anal. Chem.* **2017**, *89*, 8696−8703.
(42) Glasius, M.; Lahaniati, M.; Calogirou, A.; Di Bella, D.; Jensen, N. R.; Hjorth, J.; Kotzias, D.; Larsen, B. R. Carboxylic Acids in Secondary Aerosols from Oxidation of Cyclic Monoterpenes by Ozone. *Environ. Sci. Technol.* **2000**, *34*, 1001−1010.
(43) Yu, J.; Cocker, D. R., III; Griffin, R. J.; Flagan, R. C.; Seinfeld, J. H. Gas-Phase Ozone Oxidation of Monoterpenes: Gaseous and Particulate Products. *J. Atmos. Chem.* **1999**, *34*, 207−258.
(44) Yu, J.; Flagan, R. C.; Seinfeld, J. H. Identification of Products Containing −COOH, −OH, and −CO in Atmospheric Oxidation of Hydrocarbons. *Environ. Sci. Technol.* **1998**, *32*, 2357−2370.
(45) Yasmeen, F.; Szmigielski, R.; Vermeylen, R.; Gómez-González, Y.; Surratt, J. D.; Chan, A. W. H.; Seinfeld, J. H.; Maenhaut, W.; Claeys, M. Mass spectrometric characterization of isomeric terpenoic acids from the oxidation of α-pinene, β-pinene, d-limonene, and Δ3-carene in fine forest aerosol. *J. Mass Spectrom.* **2011**, *46*, 425−442.
(46) Claeys, M.; Iinuma, Y.; Szmigielski, R.; Surratt, J. D.; Blockhuys, F.; Van Alsenoy, C.; Böge, O.; Sierau, B.; Gómez-González, Y.; Vermeylen, R.; Van der Veken, P.; Shahgholi, M.; Chan, A. W. H.; Herrmann, H.; Seinfeld, J. H.; Maenhaut, W. Terpenylic Acid and Related Compounds from the Oxidation of α-Pinene: Implications for New Particle Formation and Growth above Forests. *Environ. Sci. Technol.* **2009**, *43*, 6976−6982.
(47) Kahnt, A.; Vermeylen, R.; Iinuma, Y.; Safi Shalamzari, M.; Maenhaut, W.; Claeys, M. High-molecular-weight esters in α-pinene ozonolysis secondary organic aerosol: structural characterization and mechanistic proposal for their formation from highly oxygenated molecules. *Atmos. Chem. Phys.* **2018**, *18*, 8453−8467.
(48) Iinuma, Y.; Ramasamy, S.; Sato, K.; Kołodziejczyk, A.; Szmigielski, R. Structural Characterisation of Dimeric Esters in α-Pinene Secondary Organic Aerosol Using N2 and CO2 Ion Mobility Mass Spectrometry. *Atmosphere* **2021**, *12*, No. 17.
(49) Ye, P.; Ding, X.; Hakala, J.; Hofbauer, V.; Robinson, E. S.; Donahue, N. M. Vapor wall loss of semi-volatile organic compounds in a Teflon chamber. *Aerosol Sci. Technol.* **2016**, *50*, 822−834.
(50) Berndt, T.; Scholz, W.; Mentler, B.; Fischer, L.; Herrmann, H.; Kulmala, M.; Hansel, A. Accretion Product Formation from Self- and Cross-Reactions of RO2 Radicals in the Atmosphere. *Angew. Chem., Int. Ed.* **2018**, *57*, 3820−3824.

https://doi.org/10.1021/acs.est.2c04786
Environ. Sci. Technol. 2022, 56, 16643−16651